

Title	Structural and luminescence properties of Eu-doped ZnO nanorods fabricated by a microemulsion method. Structural and luminescence properties of Eu-doped ZnO nanorods fabricated by a microemulsion method
Author(s)	Ishizumi, Atsushi; Kanemitsu, Yoshihiko
Citation	Applied Physics Letters (2005), 86(25)
Issue Date	2005-06
URL	http://hdl.handle.net/2433/87365
Right	c 2005 American Institute of Physics.
Type	Journal Article
Textversion	publisher

Structural and luminescence properties of Eu-doped ZnO nanorods fabricated by a microemulsion method

Atsushi Ishizumi

Graduate School of Materials Science, Nara Institute of Science and Technology,
Ikoma, Nara 630-0192, Japan

Yoshihiko Kanemitsu^{a)}

International Research Center for Elements Science, Institute for Chemical Research, Kyoto University, Uji,
Kyoto 611-0011, Japan

(Received 2 September 2004; accepted 13 May 2005; published online 15 June 2005)

We have studied photoluminescence (PL) properties of Eu-doped ZnO (ZnO:Eu) nanorods fabricated by a microemulsion method. The ZnO:Eu nanorods have a hexagonal crystal structure and exhibit a sharp luminescence due to the intra-4*f* transitions of Eu³⁺ ions. The excitation energy and temperature dependence of the PL intensity show that the Eu³⁺-related PL efficiency is determined by the energy relaxation process of excited Eu³⁺ ions, rather than by the energy transfer process from ZnO nanorods to Eu³⁺ ions. The energy transfer and luminescence processes in ZnO:Eu nanorods are discussed. © 2005 American Institute of Physics. [DOI: 10.1063/1.1952576]

Recently, there have been extensive studies on optical properties of semiconductor nanocrystals due to their size- and shape-dependent optical responses.¹⁻³ In particular, high-quality II-VI semiconductor nanocrystal samples have been prepared and their luminescence properties have been studied both experimentally and theoretically.⁴⁻⁸ In addition, II-VI compound semiconductor nanocrystals are unique host materials for doping of optically active impurities, and semiconductor nanocrystals doped with luminescence centers exhibit efficient luminescence even at room temperature.^{9,10} Therefore, many different techniques have been developed to synthesize II-VI semiconductor nanocrystals doped with luminescence centers, such as transition-metal ions,⁹⁻¹² rare-earth ions,^{13,14} and donor-acceptor pairs.¹⁵

So far, investigations for the optical properties of II-VI semiconductor nanocrystals have been concentrated mostly on CdSe and CdS nanoparticles and nanorods.¹⁻⁷ However, the best-studied CdSe and CdS materials include the harmful elements such as Cd and Se. On the other hand, it is believed that ZnO is an environmentally friendly material and is one of the suitable candidates for practical use as a nanodevice material. Furthermore, ZnO nanocrystals with wide-band-gap energies have a potential as a host material for doping of luminescence centers. It has been reported that the ZnO nanocrystals doped with Eu and Mn ions were fabricated by a microemulsion method.¹⁶ Eu-doped ZnO nanocrystals exhibit the broadband luminescence in the visible spectral region at room temperature. It is speculated that the broad and visible band is due to Eu²⁺ ions in ZnO nanocrystals.¹⁶ However, the structural and luminescence properties of impurity-doped ZnO nanocrystals are not clear.

In this work, we have fabricated Eu-doped ZnO (ZnO:Eu) nanocrystals and have studied their photoluminescence (PL) properties. Transmission electron microscope (TEM) and x-ray diffraction (XRD) studies show that the ZnO nanocrystals have a rod-like shape and that their crystal structure is hexagonal. The ZnO:Eu nanorods show the sharp

luminescence related to the intra-4*f* transitions of Eu³⁺ ions under the low-energy excitation below the band-gap energy of ZnO. The PL properties and PL mechanism in ZnO:Eu nanorods are discussed.

The ZnO:Eu nanorod samples were fabricated by a microemulsion method, according to the literature.¹⁶ We prepared two identical mixtures of octane, cetyl trimethyl ammonium bromide (CTAB), and butanol. An aqueous solution of ZnCl₂ and EuCl₂ was added to one mixture, while aqueous ammonia was added to the other mixture. We then obtained two microemulsions with the aqueous solution encapsulated within the reverse micelles formed by surfactant (CTAB) and cosurfactant (butanol) in oil (octane): one contained Zn²⁺ and Eu²⁺ ions, and the other contained OH⁻ ions. After mixing the two microemulsions, nanoparticles of hydroxide of Zn and Eu were yielded and were precipitated. The weight ratio of Eu ions to Zn ions was 0.02. The hydroxide nanoparticles were extracted from solution by a centrifugation and by a stir with ultrasound in water. The nanoparticles of hydroxides were oxidized by heating at 100 °C for 60 min and were converted to ZnO:Eu nanocrystals.

The crystal structure and shape of ZnO:Eu nanocrystals were studied by XRD (Rigaku, RINT RAPID, Cu K_α) and TEM (JEOL, JEM-3100FEF, 300 kV) measurements. For PL measurements, a He-Cd laser, a GaN laser diode, and an Ar-ion laser were used as the excitation sources for various excitation energies. The PL signals from the samples were detected by a photomultiplier through a 25 cm double-grating monochromator. The signal was amplified by a lock-in amplifier. The spectral sensitivity of the measuring systems was calibrated using a tungsten standard lamp.

Figure 1(a) shows the XRD pattern of the ZnO:Eu nanocrystals fabricated by the microemulsion method. All the peaks of the XRD patterns can be indexed to ZnO with the hexagonal structure. No diffraction peaks are detected from any other products, such as europium oxides. As shown in Fig. 1(b), the rod-like ZnO:Eu nanocrystals (ZnO:Eu nanorods) are observed in the TEM image. The average lengths of the long and short axes of nanorods are ~500 and ~50 nm, respectively. The results suggest that the microemulsion

^{a)} Author to whom correspondence should be addressed; electronic mail: kanemitsu@scl.kyoto-u.ac.jp

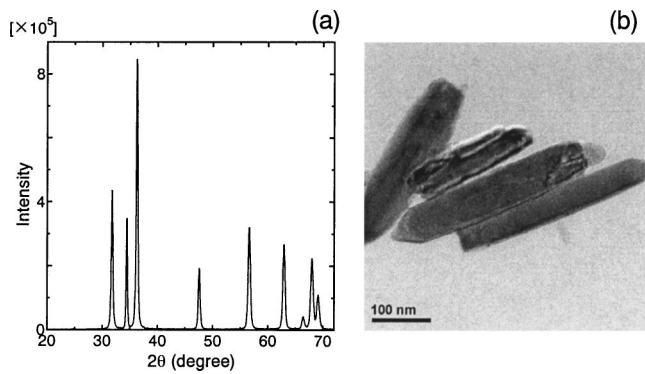


FIG. 1. XRD pattern (a) and TEM image (b) of ZnO:Eu nanorods fabricated by the microemulsion method.

method is a route for the fabrication of ZnO nanorods doped with optically active impurities.

Figure 2(a) shows the PL spectrum of ZnO:Eu nanorods under 325 nm He–Cd laser excitation at 15 K. In the PL spectrum, the emission peak is observed at ~ 370 nm, which is attributed to the bound exciton emission.¹⁷ The broad emission band is also observed around ~ 650 nm, similar to the broad PL spectrum in a previous report.¹⁶ It is known that the Eu^{2+} ions in crystals usually give a broadband emission due to the $f-d$ transition.¹⁸ We tried to confirm the existence of Eu^{2+} ions in our samples by electron spin resonance (ESR) measurements. However, we were not able to observe the ESR signals from Eu^{2+} ions in our ZnO:Eu nanorod samples. Therefore, it is believed that the observed broad PL band is attributed to defects in ZnO nanorods, rather than to Eu^{2+} ions in ZnO nanorods. On the other hand the Eu^{3+} -related PL bands are clearly observed, as will be discussed subsequently.

The PL measurements were also performed under 405 and 465.8 nm light excitation. These excitation laser energies almost coincide with the energies of the 7F_0 - 5D_3 and 7F_0 - 5D_2 transitions of Eu^{3+} ions, which are 3.02 eV (410 nm) and 2.67 eV (464 nm), respectively.^{18,19} The PL spectra under 405 and 465.8 nm light excitation are shown in Figs. 2(b) and 2(c), respectively. In these PL spectra, the sharp peaks due to the intra- $4f$ transitions of Eu^{3+} ions are clearly observed, in addition to the broad PL band related to defects of ZnO nanorods. These results imply that doped Eu^{2+} ions are converted to Eu^{3+} ions during the oxidation

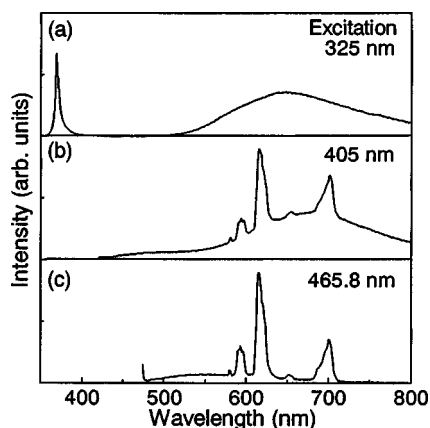


FIG. 2. PL spectra of ZnO:Eu nanorods under (a) 325, (b) 405, and (c) 465.8 nm light excitation at 15 K.

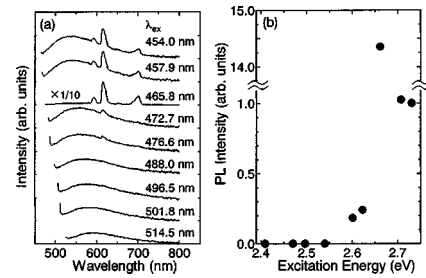


FIG. 3. (a) PL spectra of ZnO:Eu nanorods at different excitation wavelengths at 15 K. The excitation wavelengths λ_{ex} are shown in this figure. (b) Excitation energy dependence of the Eu^{3+} -related PL intensity in ZnO:Eu nanorods.

process from $\text{Zn}(\text{OH})_2$ to ZnO, because Eu^{2+} ions can be easily oxidized to Eu^{3+} ions.¹⁴

Figure 3(a) shows the PL spectra under different wavelength excitations using an Ar^+ laser at 15 K. In these spectra, the sharp PL lines due to Eu^{3+} ions are observed, in addition to the broad PL band due to defects of ZnO.²⁰ The 465.8 nm laser light can excite directly Eu^{3+} ions in ZnO nanorods (this photon energy resonantly excites the 7F_0 - 5D_2 transition of Eu^{3+} ions), while the others are nonresonant excitation (no direct excitation of Eu^{3+} ions). The Eu^{3+} -related PL intensity is clearly enhanced under 465.8 nm light excitation, although the magnitude of the resonant enhancement depends on the sample. The sharp PL peaks due to Eu^{3+} ions are also observed, even under the nonresonant excitation.

The spectrally integrated intensities of the Eu^{3+} -related PL are plotted as a function of the excitation energy in Fig. 3(b). Under the resonant excitation, the direct excitation of Eu^{3+} ions enhances the sharp luminescence of the direct intra- $4f$ transitions in Eu^{3+} ions. In addition, at the high excitation energy above the 7F_0 - 5D_2 transition energy of Eu^{3+} ions (2.67 eV), the PL intensity of Eu^{3+} ions increases. Here, in Eu^{3+} -doped solids, the excitation of the 7F_0 - 5D_2 transition of Eu^{3+} ions usually causes the red Eu^{3+} -related PL. The observation of red PL under nonresonant 2.70 and 2.73 eV excitation suggests that the excited state of Eu^{3+} ions is produced by energy transfer from the host ZnO nanorod to Eu^{3+} ions. Since these excitation energies in Fig. 3 are lower than the band-gap energy of ZnO, it is considered that the energy transfer from ZnO nanorods to Eu^{3+} ions occurs through the defects of ZnO nanorods.

The temperature dependence of the PL intensity has been studied under resonant and nonresonant excitation of the intra- $4f$ transition of Eu^{3+} ions, in order to clarify the PL and the Eu^{3+} excitation processes in ZnO:Eu nanorods. Figure 4(a) shows the temperature dependence of the Eu^{3+} -related PL intensity under 405 (solid circles), 465.8 (open circles), and 454.0 nm (solid triangles) light excitation. The 405 and 465.8 nm light excitation directly excited the 7F_0 - 5D_3 and 7F_0 - 5D_2 transitions of Eu^{3+} ions, respectively, while the 454.0 nm light is the nonresonant excitation of the intra- $4f$ transitions of Eu^{3+} ions. However, it is found that there is no significant difference in the temperature dependence of the Eu^{3+} -related PL intensity between resonant and nonresonant excitation. This observation implies that the temperature-dependent PL intensities are determined by the relaxation process of excited Eu^{3+} ions, rather than the excitation process of Eu^{3+} ions.

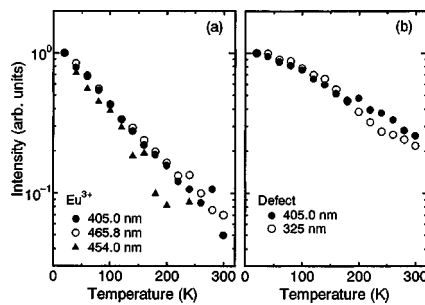


FIG. 4. Temperature dependence of (a) the Eu^{3+} -related PL intensity and (b) the defect-related PL intensity in ZnO:Eu nanorods. The PL intensity at the lowest temperature is taken as unity.

Figure 4(b) shows the temperature dependence of the defect-related PL intensity (the broad PL around 600 nm) of ZnO:Eu nanorods under 325 (open circles) and 405-nm (solid circles) light excitation. There is no significant difference in the temperature dependence of the defect-related PL intensity between 325 and 405 nm excitation. Even under 405 nm excitation (the excitation laser energy is lower than the band-gap energy of ZnO), the defects states are directly excited by the laser light and the defect-related PL is clearly observed in ZnO:Eu nanorods. If the energy transfer rate from defects to Eu^{3+} ions determines the efficiency of the Eu^{3+} -related PL, it is expected that the temperature dependence of the Eu^{3+} -related PL intensity is similar to that of the defect-related PL intensity, because the Eu^{3+} -related PL intensity is proportional to the number of the photogenerated carriers trapped at the defects of ZnO nanorods. However, the temperature dependence of the Eu^{3+} -related PL intensity is different from that of the defect-related PL in ZnO:Eu nanorods: The Eu^{3+} -related PL intensity decreases faster than the defect-related PL intensity with an increase of temperature. Therefore, it is concluded that the efficiency of the Eu^{3+} -related PL is determined by the nonradiative process of excited Eu^{3+} ions. It is believed that the defects are formed around the trivalent Eu^{3+} ions in the II-VI compound ZnO nanorods and the defects in nanorods affect the energy relaxation process of excited Eu^{3+} ions.

In conclusion, we have studied PL properties of Eu-doped ZnO nanorods fabricated by the microemulsion method. The bound exciton-related PL is observed near 370 nm in ZnO:Eu nanorods under the 325 nm light excitation. The PL peaks due to the intra- $4f$ transition of Eu^{3+} ions

are also observed under the low-energy excitation below the band-gap energy of ZnO. From the excitation energy and temperature dependence of the Eu^{3+} -related PL intensity, it is concluded that the energy transfer occurs from the ZnO nanorods to Eu^{3+} ions through defect states and the efficiency of the Eu^{3+} -related PL intensity is determined by the nonradiative process of excited Eu^{3+} ions in ZnO nanorods.

This work was supported in part by a Grant-in-Aid for Scientific Research (KAKENHI, 14340093) from the Japan Society for the Promotion of Science, The Research Foundation for Opto-Science and Technology, and The Futaba Electronics Memorial Foundation.

- ¹See, for example, L. E. Brus, Al. L. Efros, and T. Itoh, *J. Lumin.* **70**, 1 (1996).
- ²X. Peng, L. Manna, W. Yang, J. Wickham, E. Scher, A. Kadavanich, and A. P. Alivisatos, *Nature (London)* **404**, 59 (2000).
- ³J. Hu, L.-S. Li, W. Yang, L. Manna, L.-W. Wang, and A. P. Alivisatos, *Science* **292**, 2060 (2001).
- ⁴C. B. Murray, D. J. Norris, and M. G. Bawendi, *J. Am. Chem. Soc.* **115**, 8706 (1993).
- ⁵N. Nirmal, B. O. Dabbousi, M. G. Bawendi, J. I. Macklin, J. K. Trautman, T. D. Harris, and L. E. Brus, *Nature (London)* **383**, 802 (1996).
- ⁶S. A. Empedocles, D. J. Norris, and M. G. Bawendi, *Phys. Rev. Lett.* **77**, 3873 (1996).
- ⁷D. Matsuura, Y. Kanemitsu, T. Kushida, C. W. White, J. D. Budai, and A. Meldrum, *Appl. Phys. Lett.* **77**, 2289 (2000).
- ⁸Al. L. Efros and M. Rosen, *Phys. Rev. Lett.* **78**, 1110 (1997).
- ⁹R. N. Bhargava, D. Gallagher, X. Hong, and A. Nurmikko, *Phys. Rev. Lett.* **72**, 416 (1994).
- ¹⁰A. A. Bol and A. Meijerink, *Phys. Rev. B* **58**, R15997 (1998); *Phys. Status Solidi B* **224**, 291 (2001).
- ¹¹M. Tanaka, *J. Lumin.* **100**, 163 (2002).
- ¹²Y. Kanemitsu, H. Matsubara, and C. W. White, *Appl. Phys. Lett.* **81**, 535 (2002).
- ¹³S. Okamoto, M. Kobayashi, Y. Kanemitsu, and T. Kushida, *Phys. Status Solidi B* **229**, 481 (2002).
- ¹⁴W. Chen, J.-O. Malm, V. Zwiller, Y. Huang, S. Liu, R. Wallenberg, J.-O. Bovin, and L. Samuelson, *Phys. Rev. B* **61**, 11021 (2000).
- ¹⁵A. Ishizumi, C. W. White, and Y. Kanemitsu, *Appl. Phys. Lett.* **84**, 2397 (2004).
- ¹⁶R. N. Bhargava, V. Chhabra, T. Som, A. Ekimov, and N. Taskar, *Phys. Status Solidi B* **229**, 897 (2002); V. Chhabra, B. S. Kulkarni, and R. N. Bhargava, U.S. Patent No. 6,036,886 (14 March 2000).
- ¹⁷D. C. Reynolds, D. C. Look, B. Jogai, C. W. Litton, T. C. Collins, W. Harsch, and G. Cantwell, *Phys. Rev. B* **57**, 12151 (1998).
- ¹⁸See, for example, *Phosphor Handbook*, edited by S. Shionoya and W. M. Yen (CRC Press, Boca Raton, FL, 1999).
- ¹⁹G. H. Dieke and H. M. Crosswhite, *Appl. Opt.* **2**, 675 (1963).
- ²⁰X. L. Wu, G. G. Siu, C. L. Fu, and H. C. Ong, *Appl. Phys. Lett.* **78**, 2285 (2001).